

RESEARCH

Open Access



Genome-wide identification, tissue expression pattern, and salt stress response analysis of the NAC gene family in *Thinopyrum elongatum*

Jilin Sun^{1†}, Xiaokuo Cui^{2†}, Jiaqi Zhang¹, Fansen Meng¹, Jiangong Li¹, Shenghui Zhou³, Changai Wu², Peng Zhou³, Silong Sun¹ and Long Han^{4*}

Abstract

Background The NAC (NAM, ATAF1/2, and CUC2) gene family plays a critical role in regulating plant growth, developmental processes, and stress response mechanisms. While NAC genes have been systematically characterized in multiple plant species, this study focused on genome-wide identification of NAC family members in *Thinopyrum elongatum* (designated as *TeNACs*) through integrated bioinformatics approaches. Comprehensive analyses were conducted to determine the physicochemical characteristics, conserved motifs, gene structure, phylogenetic relationships, chromosomal collinearity, and expression profiles of the identified *TeNACs*. This multi-dimensional characterization provides fundamental insights into the structural and functional diversity of NAC transcription factors in *Th. elongatum*.

Results A total of 116 NAC transcription factors were systematically identified in *Th. elongatum*, distributed across all seven chromosomes. Comprehensive physicochemical characterization revealed substantial variation among *TeNAC* proteins: amino acid length (162–718 aa), molecular weight (18.33–78.25 kDa), isoelectric point (6.5–7.5), instability index (30.34–63.32), and aliphatic index (50.92–80.68). Hydropathicity analysis confirmed the hydrophilic nature of all *TeNACs*, with grand average values consistently below zero. Conserved motif profiling demonstrated a highly conserved architecture in *TeNACs*, featuring ordered arrangements of motifs 3, 4, 1, 5, 6, 2, and 7. Phylogenetic reconstruction classified *TeNACs* into 14 distinct clades through comparative analysis with *Arabidopsis thaliana* NAC genes, notably lacking ANAC001 and OsNAC8 homologs. Comparative genomic analysis identified significant syntenic conservation between *TeNACs* and wheat NAC genes. Protein interaction network prediction indicated intricate functional associations among *TeNAC* proteins. Computational predictions coupled with experimental validation of *TeNAC021* confirmed exclusive nuclear localization for all family members. Differential expression analysis across a salt gradient (0–300 mM) identified 14 *TeNACs* with progressive up-regulation and 5 showing consistent down-regulation. RT-qPCR confirmed salt-responsive expression patterns for eight *TeNACs* demonstrating marked transcriptional changes.

[†]Jilin Sun and Xiaokuo Cui contributed equally to this work.

*Correspondence:

Long Han

hanlonghello2008@163.com

Full list of author information is available at the end of the article



Conclusions This systematic investigation establishes a robust theoretical framework for subsequent structural and functional characterization of *TeNACs* in *Th. elongatum*.

Keywords *TeNACs*, *Th. elongatum*, Expression pattern, Salt stress

Introduction

The NAC family represents a crucial plant-specific gene family, deriving its name from the first letters of three foundational subfamilies: non-apical meristem (NAM) initially characterized in *Petunia*, along with transcription factor ATAF1/2 and CUC2 (cup-shaped cotyledon) subsequently identified in *Arabidopsis*. These evolutionarily conserved transcription factors share a highly conserved N-terminal DNA-binding domain while maintaining divergent C-terminal regions [1, 2]. The NAM domain (150–160 amino acids), situated at the N-terminal region of NAC transcription factors, consists of a highly conserved protein sequence. This sequence serves as a critical binding site for NAC transcription factors to interact with the promoters of target genes, forming a fundamental basis for identifying the NAC gene family. In contrast, the C-terminal domain of NAC transcription factors contains diverse protein sequences, which is involved in regulating the transcription of downstream target genes [3]. The N-terminal conserved domain of NAC transcription factors can be divided into five distinct subdomains: A, B, C, D, and E. Among these subdomains, A, C, and D show high conservation, while B and E display moderate conservation. Subdomain A is mainly involved in dimer binding and formation, whereas subdomains C and D are responsible for DNA sequence recognition. In contrast, subdomains B and E play crucial roles in determining the functional diversity of the NAC gene family [4].

The NAC gene family plays essential roles in plant growth and development, including apical meristem formation [5], floral organ development [6], fruit maturation [7], leaf senescence [8], secondary cell wall formation [9] and root development [10]. Furthermore, NAC transcription factors positively or negatively regulate responses to abiotic stresses, including salinity [11], low temperature [12], and drought [13], that plants face during growth and development. Previous studies have demonstrated that overexpression of *ONAC066* and *TwNAC01* improved drought stress responses in rice (*Oryza sativa*) and *Triticale*, respectively. Conversely, suppression of *TwNAC01* reduced the net photosynthetic rate, stomatal conductance, intercellular CO₂ concentration, and transpiration rate in *Triticocoscale wittmack* leaves [14, 15]. The role of *LINAC2* in *Lilium lancifolium* under abiotic stress is not limited to low temperature, drought, and salt stress responses, as its expression is also induced upon

exposure to abscisic acid (ABA) signaling molecules [16]. In *Triticum aestivum*, *TaNAC29* is a key regulator of abiotic stress signaling pathways and antioxidant systems, decreasing H₂O₂ accumulation and membrane damage for enhanced salt tolerance [17]. In *O. sativa*, *OsNAC3* plays a crucial role in ABA responses and salt tolerance through regulating the expression of stress-related genes and maintaining Na⁺ homeostasis in rice stems. Additionally, *ONAC127* and *ONAC129* control grain filling by influencing sugar transport and abiotic stress responses [18, 19]. Furthermore, overexpression of *GmNAC06* markedly improves salt tolerance in soybean (*Glycine max*) hairy roots, while *GmNAC12* functions as a key regulator that positively modulates drought tolerance [20].

Thinopyrum elongatum (Host) D.R.Dewey (EE, 2n = 2x = 14) is a perennial plant in the tribe *Triticeae* with excellent characteristics including disease resistance, high fertility, and multiple stress tolerances, particularly to drought, low temperature, and salinity. Moreover, *Th. elongatum* is phylogenetically closely related to common wheat and harbors numerous valuable genes that have been effectively utilized in wheat genetic improvement [21, 22]. To investigate the tissue-specific expression patterns and elucidate the salt tolerance mechanisms of the NAC genes in *Th. elongatum*, a comprehensive study was conducted. In this study, we utilized bioinformatics approaches to perform genome-wide identification of the *TeNACs*. Furthermore, we systematically analyzed the physicochemical properties, conserved motifs, gene structure, evolutionary relationships, collinearity, protein–protein interactions, and other relevant characteristics. Additionally, we examined the expression patterns under salt stress and across different tissues. Our findings establish a theoretical foundation for further research on the biological functions and molecular mechanisms of the *TeNACs*.

Materials and methods

Identification and physicochemical property analysis of the *TeNACs* family

The protein sequences of NAC genes in *A. thaliana* and the genome/annotation files of *Th. elongatum* were retrieved from TAIR (<https://www.arabidopsis.org/>) and Genome Warehouse (<https://ngdc.cnbc.ac.cn/gwh/Assembly/965/show>), respectively. Two complementary methods were employed to identify *TeNAC* members.

The first method involved performing BLASTP (v2.13.0) analysis using the *A. thaliana* NAC protein sequences as queries with an e-value cutoff of $1e^{-20}$ to screen and classify *Th. elongatum* protein sequences. The second method utilized HMMER (v3.3.2) to build a hidden Markov model profile with the same e-value threshold ($1e^{-20}$), enabling identification of candidate sequences in *Th. elongatum* using the NAM (PF02365) domain from Pfam (<http://pfam-legacy.xfam.org/>). The candidate sequences obtained from both methods were then submitted to NCBI CDD (<https://www.ncbi.nlm.nih.gov/Structure/bwrpsb/bwrpsb.cgi>) and InterPro (<https://www.ebi.ac.uk/interpro/search/sequence/>) databases for precise NAC domain verification. Following stringent screening and validation procedures, the final gene set was obtained and systematically named according to their Latin nomenclature and genomic locations. The fundamental physicochemical parameters of the identified TeNAC proteins, including protein length, molecular weight, theoretical isoelectric point (pI), instability index, aliphatic index, and grand average of hydropathicity (GRAVY), were analyzed using ExPASy (<https://web.expasy.org/protparam/>) [23].

Genomic distribution and collinearity analysis

TBtools (v1.120) software was employed to visualize the chromosomal distribution of *TeNACs* [24]. To examine the collinearity relationships of *TeNACs* both within and across species, genome sequences of *A. thaliana*, *O. sativa*, and *T. aestivum* were obtained from TAIR, RGAP (<http://rice.plantbiology.msu.edu/>), and IWGSC (<https://wheat-urgi.versailles.inra.fr/Projects/IWGSC>), respectively. Interspecies and intraspecies collinearity analyses were conducted using MCscanX, with the resulting collinearity networks visualized through TBtools.

Conserved motif, cis-acting elements, and gene structure analyses

The conserved motifs and gene structures of *TeNACs* were systematically characterized using MEME (v5.5.3) (<https://meme-suite.org/meme/tools/meme>) and TBtools, respectively [25]. Subsequently, the 2,000 bp upstream sequences of *TeNACs* were extracted and submitted to PlantCARE (<https://bioinformatics.psb.ugent.be/webtools/plantcare/html/>) for cis-acting element prediction. TBtools was employed to visualize the conserved motifs, cis-acting elements, and gene structures. The maximum number of motifs was set to 10, while default parameters were maintained for other settings.

Prediction of protein-protein interactions in *TeNACs*

STRING (<https://cn.string-db.org/>) was used to predict the interactions of the *TeNAC* proteins, with *T. aestivum*

as the selected organism and 116 *TeNAC* proteins as a reference for predicting protein–protein interactions [26].

Evolutionary analysis

MAFFT (v7.520) was used to compare the amino acid sequences of the identified *TeNACs* with those of *A. thaliana* NAC genes [27]. The resulting data were used to construct a phylogenetic tree using IQ-TREE (v2.2.2.7) with maximum likelihood algorithm and 1000 bootstrap replicates. The online website iTOL (<https://itol.embl.de/>) was used to visualize the phylogenetic tree [28].

Subcellular localization prediction and *TeNAC021* validation

The subcellular localization of *TeNACs* was determined using Cell-PLoc 2.0 (<http://www.csbio.sjtu.edu.cn/bioinf/Cell-PLoc-2/>) [29]. It was predicted that *TeNAC021* might be located in both chloroplasts and nucleus, so experimental validation was employed. The coding region of *TeNAC021* was amplified using the following primers: Forward primer (5′–3′) ATGGCATCGGCA GCGTTA and Reverse primer (5′–3′) GTTTTTTTT TTTAGCAAACGTGATG. The PCR product was then cloned into the pCAMBIA1305-eGFP vector, which was fused to a GFP protein in the C terminus using the KpnI and BamHI restriction sites by the In-Fusion reaction. Then, the fusion vector was transformed to the p19 containing *Agrobacterium* strain GV3101 (pSoup-p19). The Ubi::TeNAC21-GFP was expressed in *Nicotiana benthamiana* leaves by agro-infiltration. Images were collected on a confocal microscope (LSM900, Zeiss, Germany). GFP was detected at 488 nm laser excitation and collection bandwidth was 510–550 nm.

Sequencing and analyses of the transcriptome of *Th. elongatum*

The seeds of *Th. elongatum* (PI 531718) were obtained from United States Department of Agriculture (USDA) National Plant Germplasm System (<https://npgsweb.ars-grin.gov/gringlobal/accessiondetail?id=1426654>). The plants were cultivated in a growth chamber at Shandong Agricultural University (Tai'an, China), under conditions of 25 °C and a 16 h/8 h (light/dark) photoperiod. Thereafter, the plants were treated with salt at different concentrations (0, 100, 200, and 300 mM NaCl). After one week treatment, leaf tissue samples of *Th. elongatum* were collected and stored at –80 °C in liquid nitrogen. The RNAprep Pure Plant Kit (TIANGEN, Beijing, China) was used to extract the RNA from all samples. The NanoDrop 1000 spectrophotometer was used to measure its quantity. In total, four salt treatment groups with 3 biological replicates for each, were subjected to transcriptome

sequencing, and 372 Gb datasets were generated. To analyze the expression pattern of *TeNACs*, total RNA was extracted from the seedling, root, internode, and flag leaf tissues. Three biological replicates were performed for each tissue. RNA extraction was conducted using the TRIzol[®] reagent (Invitrogen). Sequencing was performed on the Illumina HiSeq 4000 platform. In addition, the transcriptome data of six tissues (half-grain, grain, young spike, flowering, ovary expansion, and pre-flowering) of *Th. elongatum* we previously produced, were downloaded from NCBI database (accession number PRJNA540081). About 932 Gb datasets were used to perform the tissue expression analyses.

RNA-seq data was then subjected to quality control using fastqc (v0.12.1) with the default parameters [30]. Subsequently, HISAT2 (v2.2.1) was used to align RNA-seq reads onto the reference genome of *Th. elongatum*. Finally, HTseq-count (v2.0.2) was used to generate per-gene read count for each sample [31, 32]. The transcripts per million (TPM) value for each gene was calculated based on its length and expressed as $\log_2(\text{TPM} + 1)$ using a custom R script. The resulting tables were then visualized using the HeatMap module of TBtools.

RT-qPCR analysis of the *TeNACs*

The 7-day seedlings of *Th. elongatum* were exposed to 0, 100, 200, and 300 mM NaCl for 7-day, respectively. These seedlings were then collected and stored at -80°C . The Beacon Designer tool was used to design specific primers based on the sequences of the coding regions of 8 *TeNACs*. Subsequently, the total RNA was extracted using RNA prep Pure Plant Plus Kit (DP441, TIANGEN, Beijing, Chain) from seedlings. For the first-strand cDNA synthesis, 1 μg of total RNA was used with the PrimeScript[™] II 1st Strand cDNA Synthesis Kit (6210 A, TaKaRa, Beijing, Chain). Using the three-step program on the Archimed Real-time PCR Determination System (ROCGENE, Beijing, Chain), the RT-qPCR analysis was carried out using the qPCR Super mix SYBRgreen (MF013-01, Mei5bio, Beijing, Chain). As an internal control, the *TeTublin* was employed (Forward primer (5'–3') GTGGAAGCTGGCTCTGGC and Reverse primer (5'–3') CGCTCAATGTCAAGGGA). Three biological replicates of the qPCR data were analyzed using the $2^{-\Delta\Delta\text{CT}}$ technique. A one-way ANOVA was used to determine statistical significance at a significance level of $P < 0.05$ (The sequences of specific primers are listed in Supplementary Table 1).

Results

Identification of *TeNAC* members, genomic distribution and analysis of physicochemical properties

A total of 116 NAC transcription factors were identified in *Th. elongatum* and designated as *TeNAC001-TeNAC116* based on their Latin nomenclature and genomic positions across seven chromosomes (Supplementary Table 2). Chromosomal distribution analysis showed balanced allocation of all 116 *TeNAC* members among the seven chromosomes. Chromosome 7E contained the highest number (28 *TeNACs*), while chromosome 1E had the fewest (7 genes). The distribution pattern was as follows: chromosome 2E (24), chromosome 3E (14), chromosome 4E (13), chromosome 5E (15), and chromosome 6E (16). Multiple tandem duplication events were observed among *TeNAC* members, indicating their crucial role in gene family expansion (Fig. 1A).

The *TeNAC* proteins varied in length from 162 to 718 amino acids, with molecular weights ranging between 18.33–78.25 kDa and theoretical pI spanning 4.44–9.84. Based on pI values: 47 acidic proteins (pI < 6.5), 49 basic proteins (pI > 7.5), and 20 neutral proteins (pI 6.5–7.5) were identified, showing balanced distribution between acidic and basic groups (Fig. 1B). Instability indices ranged from 30.34 to 63.32, with 90/116 (77.6%) exceeding 40. Aliphatic indices (50.92–80.68) reflected significant variation in thermal stability. All grand average of hydropathicity (GRAVY) values were negative, confirming strong hydrophilic characteristics (Fig. 1C, Supplementary Table 3).

Collinearity analyses of *TeNACs*

The collinearity analysis of *TeNACs* identified seven intra-family duplicated gene pairs (Fig. 1D), specifically between *TeNAC004-TeNAC043*, *TeNAC007-TeNAC041*, *TeNAC013-TeNAC051*, *TeNAC014-TeNAC050*, *TeNAC011-TeNAC060*, *TeNAC024-TeNAC082*, and *TeNAC021-TeNAC080*. These findings strongly support the crucial contribution of gene duplication events to *TeNAC* family expansion. Interspecies collinearity analysis showed limited synteny with *A. thaliana* (4 collinear blocks) but extensive conservation with *O. sativa* (76 collinear blocks), revealing closer evolutionary relationships with rice. We further identified 201 collinear genes across wheat A, B, and D subgenomes corresponding to 79 *TeNACs*, with detailed distribution as follows: 70 in subgenome A, 65 in subgenome B, and 66 in subgenome D, confirming strong orthologous relationships between *TeNACs* and wheat genomes (Fig. 1E).

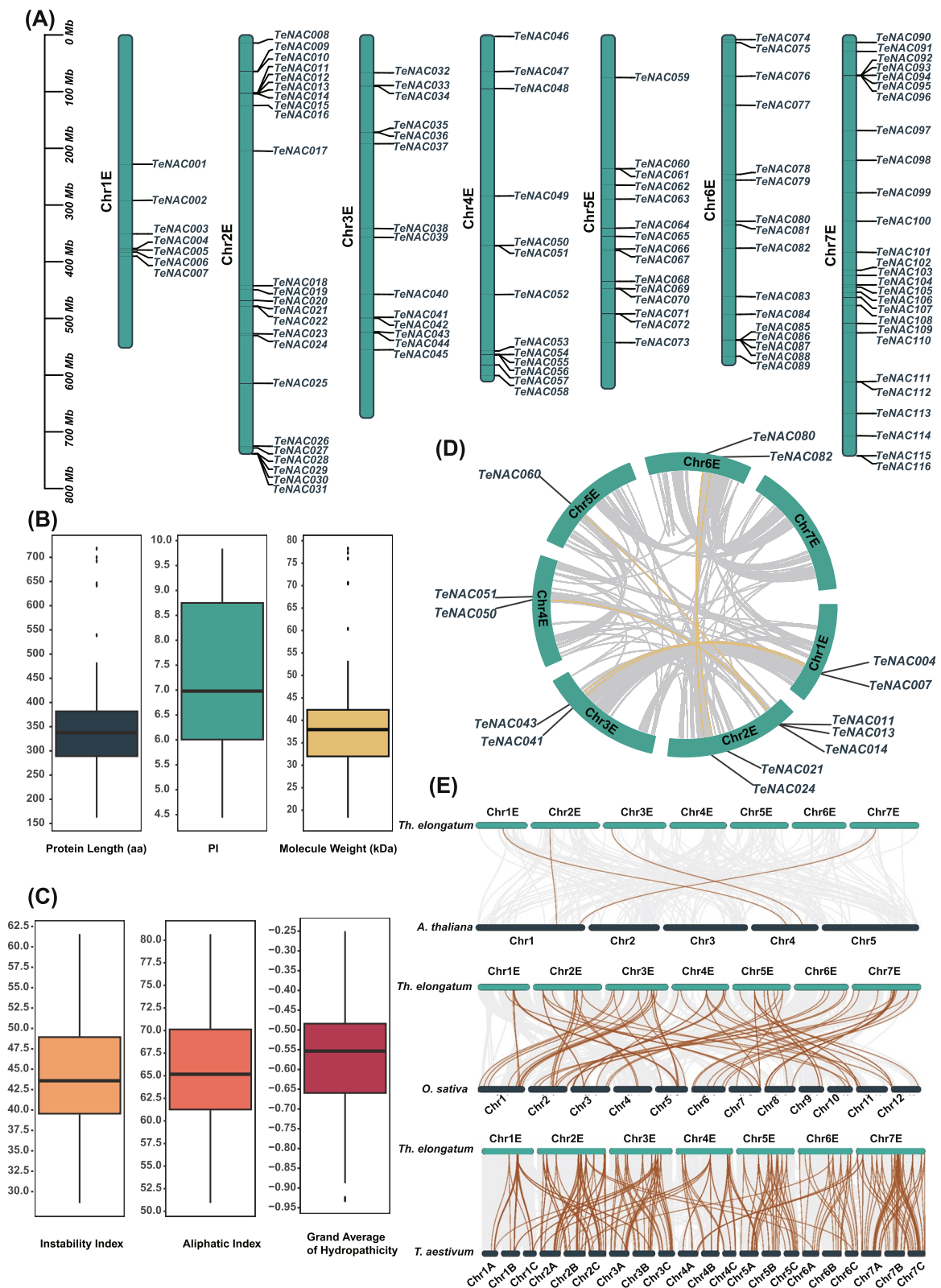


Fig. 1 The distribution, physicochemical properties, and collinearity analysis of TeNACs. **A** The distribution of TeNACs on seven chromosomes 1E to 7E of *Th. elongatum*. **B**, **C** The box plot of protein length, isoelectric point (PI), molecular weight, instability index, aliphatic index, and grand average of hydropathicity in TeNACs. **D** The intraspecific collinearity of TeNACs in *Th. elongatum*. **E** The interspecific collinearity between *A. thaliana*, *O. sativa*, *T. aestivum*, and *Th. elongatum*, respectively

Conserved motif, cis-acting elements, and gene structure analyses

Ten conserved motifs were identified in the *TeNACs* (Fig. 2A). Among these, motif 3 represents NAC subdomain A, motif 4 represents subdomain B, motif 1 represents subdomain C, motif 2 represents subdomain D, and motif 7 represents subdomain E (Supplementary Fig. 1). 102 out of all 116 *TeNACs* contained motifs 1–7. Notably, the seven conserved motifs were consistently arranged in the sequences of motifs 3, 4, 1, 5, 6, 2, and 7. This arrangement underscores the high conservation of motifs 1–7 throughout the evolutionary history of *TeNACs*. Among the remaining 14 members, *TeNAC039* does not contain motif 3; *TeNAC083* does not contain motif 4; *TeNAC018*, *TeNAC045*, and *TeNAC114* do not contain motif 1; *TeNAC005*, *TeNAC044*, and *TeNAC048* do not contain motif 6; *TeNAC021* and *TeNAC045* do not contain motif 2; and *TeNAC027* and *TeNAC074* do not contain motif 7. Motifs 8–10 were only identified in a subset of members with similar gene structure. All *TeNAC* members contain the NAM (PF02365) domain (Fig. 2B).

By identifying and screening the cis-acting elements in the 2,000 bp upstream sequence of *TeNACs*, a total of 15 elements related to hormones, stress and development were discovered (Fig. 2C). The hormone response-related elements include auxin-responsive element (TGA-element, AuxRR-core), gibberellin-responsive element (TATC-box, P-box, GARE-motif), MeJA-responsiveness (TGACG-motif, CGTCA-motif), salicylic acid responsiveness (TCA-element), and abscisic acid responsiveness (ABRE). The stress response-related elements include defense and stress responsiveness (TC-rich repeats), low-temperature responsiveness (LTR), and drought-inducibility (MBS). This indicates that the upstream region of *TeNACs* is rich and diverse in cis-acting elements. The *TeNACs* with similar gene structures had a similar number of exons and gene structures (Fig. 2D).

Protein–protein interactions

Protein–protein interaction analysis revealed four distinct interaction networks among 32 *TeNAC* members, comprising 19, 7, 4, and 2 proteins respectively (Fig. 2E–H). Notably, six central members (*TeNAC027*, *TeNAC085*, *TeNAC086*, *TeNAC087*, *TeNAC088*, and *TeNAC103*)

within the 19-member network demonstrated interactions with all 11 peripheral members, indicating intricate regulatory relationships within the *TeNAC* family (Supplementary Table 4).

Evolutionary analysis

To elucidate the evolutionary relationships of *TeNAC* members, a phylogenetic tree was generated using 105 *Arabidopsis* NAC genes along with all 116 *TeNAC* proteins (Fig. 3). Classification based on *Arabidopsis* NAC protein domains grouped the *TeNACs* into 14 distinct clades. Notably, two clades (ANAC001 and OsNAC8) lacked *TeNAC* representatives, implying potential gene loss events in *Th. elongatum* during evolution. The remaining 12 clades contained both *A. thaliana* and *Th. elongatum* NAC genes, demonstrating strong evolutionary conservation across these NAC family members. Subsequent collinearity analysis further confirmed that these 11 members lacked syntenic counterparts in the *Th. elongatum* genome assembly (Supplementary Fig. 2).

Subcellular localization

Subcellular localization prediction suggests that all 116 *TeNAC* proteins, with the exception of *TeNAC021*, which may be localized in either the chloroplast or the nucleus, are predominantly nuclear-localized. To confirm the subcellular localization of *TeNAC021*, we conducted an experimental validation. The results confirmed that *TeNAC021* is indeed localized in the nucleus (Fig. 4A).

TeNACs expression patterns in different tissues

Thirty-five *TeNAC* transcription factors exhibited constitutive expression across all examined tissues, while 69 displayed tissue-preferential expression profiles, with *TeNAC073*, *TeNAC048*, *TeNAC044*, and *TeNAC045* showing consistently high transcript abundance in all tissues (Fig. 4B, Supplementary Table 5), suggesting their fundamental regulatory roles in developmental processes in *Th. elongatum*. In contrast, twelve *TeNAC* family members (*TeNAC034*, *TeNAC038*, *TeNAC049*, *TeNAC052*, *TeNAC062*, *TeNAC063*, *TeNAC078*, *TeNAC079*, *TeNAC081*, *TeNAC084*, *TeNAC102*, and *TeNAC112*) remained transcriptionally silent across all ten investigated tissues, indicating various functions of these *TeNACs*.

(See figure on next page.)

Fig. 2 Conserved motifs, domain, cis-acting elements, gene structure, and protein–protein interaction networks of *TeNACs*. **A** Evolutionary trees and conserved motifs among *TeNACs*. Different colored blocks in the figure represent the locations of different motifs. **B** The location of the NAM domain on *TeNACs*. **C** The location distribution of homeopathic elements at 2000 bp upstream of *TeNACs*. **D** The structural features of CDS and UTR genes were distributed on *TeNACs*. (E–H) Four networks of protein–protein interaction in *TeNACs* based on *T. aestivum*. The lines between balls of different colors are evidence of an interaction between the two *TeNACs*

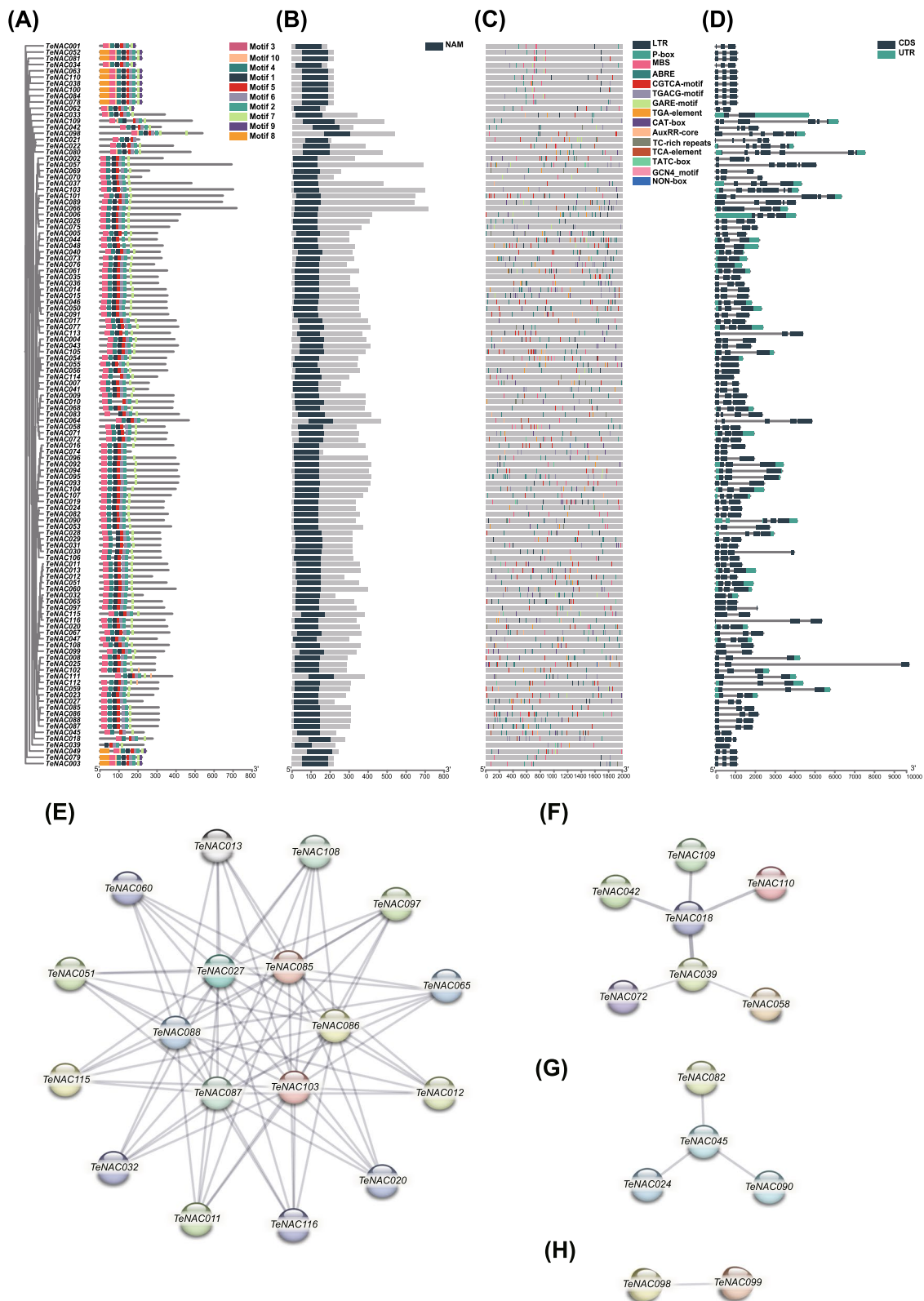


Fig. 2 (See legend on previous page.)

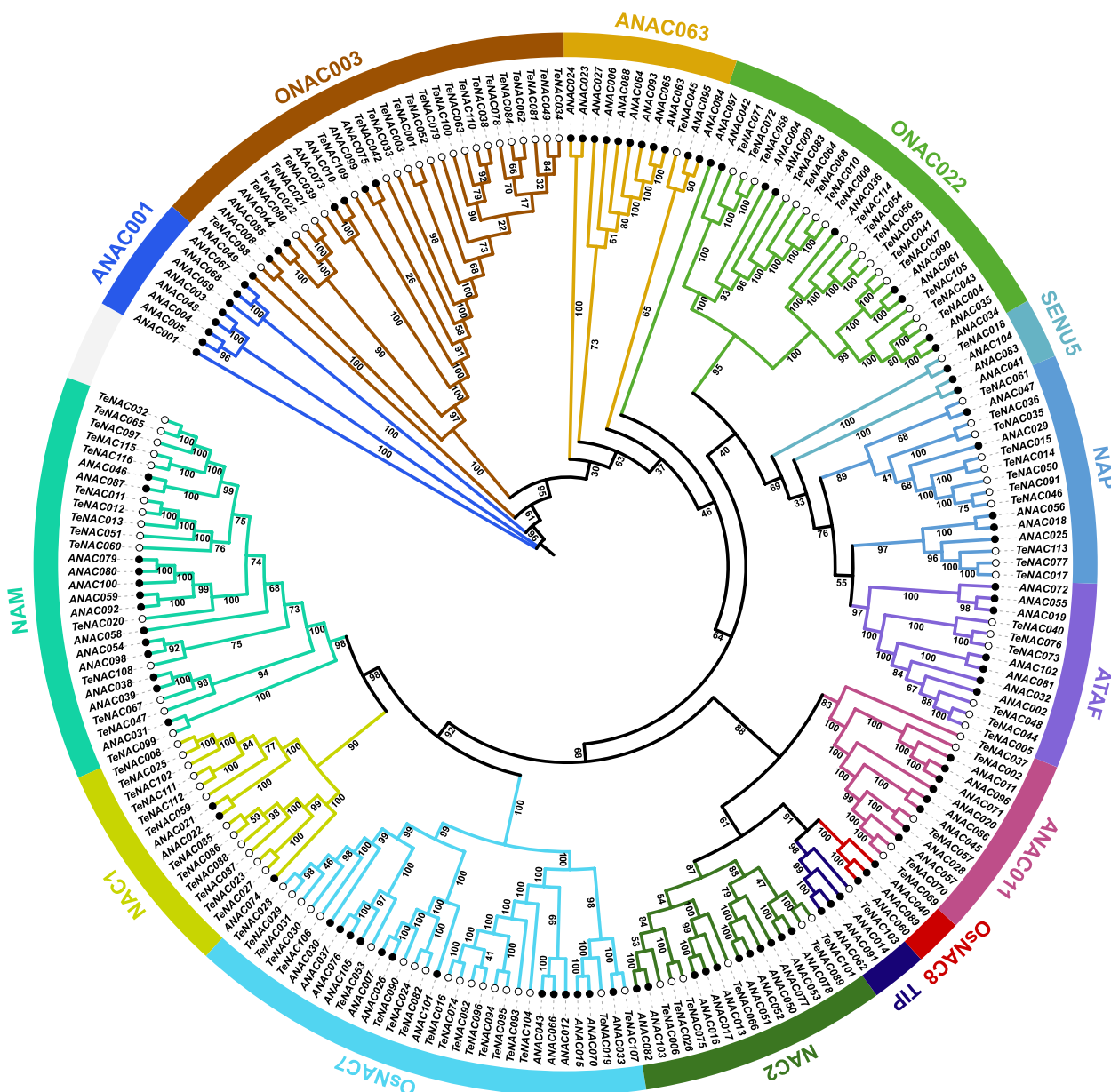


Fig. 3 Phylogenetic tree of *TeNACs* and the *A. thaliana* NAC family

Expression analysis and RT-qPCR of *TeNACs* under salt stress
 RNA-seq analysis detected expression of 91 out of 116 *TeNACs* under stress conditions (Fig. 5A, Supplementary Table 6). Specifically, *TeNAC006*, *TeNAC105*, *TeNAC103*, *TeNAC080*, *TeNAC100*, *TeNAC039*, *TeNAC033*, *TeNAC007*, *TeNAC025*, *TeNAC013*, *TeNAC029*, *TeNAC083*, *TeNAC042*, and *TeNAC098* showed sustained up-regulation. At the same time, *TeNAC005*, *TeNAC061*, *TeNAC114*, *TeNAC021*, and *TeNAC020* exhibited progressive down-regulation (Fig. 5B). These differential expression patterns demonstrate that *TeNACs* employ distinct transcriptional responses to salt stress to maintain essential physiological processes in plants.

Notably, *TeNAC073*, *TeNAC048*, *TeNAC044*, and *TeNAC045* were highly expressed in all tissues and under salt stress conditions. This suggests that they play vital regulatory roles in tissue development and salt stress responses in *Th. elongatum*. Based on the expression patterns of *TeNACs* under varying salt concentrations, we selected 4 up-regulation continuous, 2 down-regulation continuous, and 2 non-regulation continuous genes for RT-qPCR validation (Supplementary Table 7). Quantitative real-time PCR (RT-qPCR) investigations were performed to evaluate the expression patterns of these genes under various salt stress conditions. The RT-qPCR results showed consistent variations to the transcriptome data

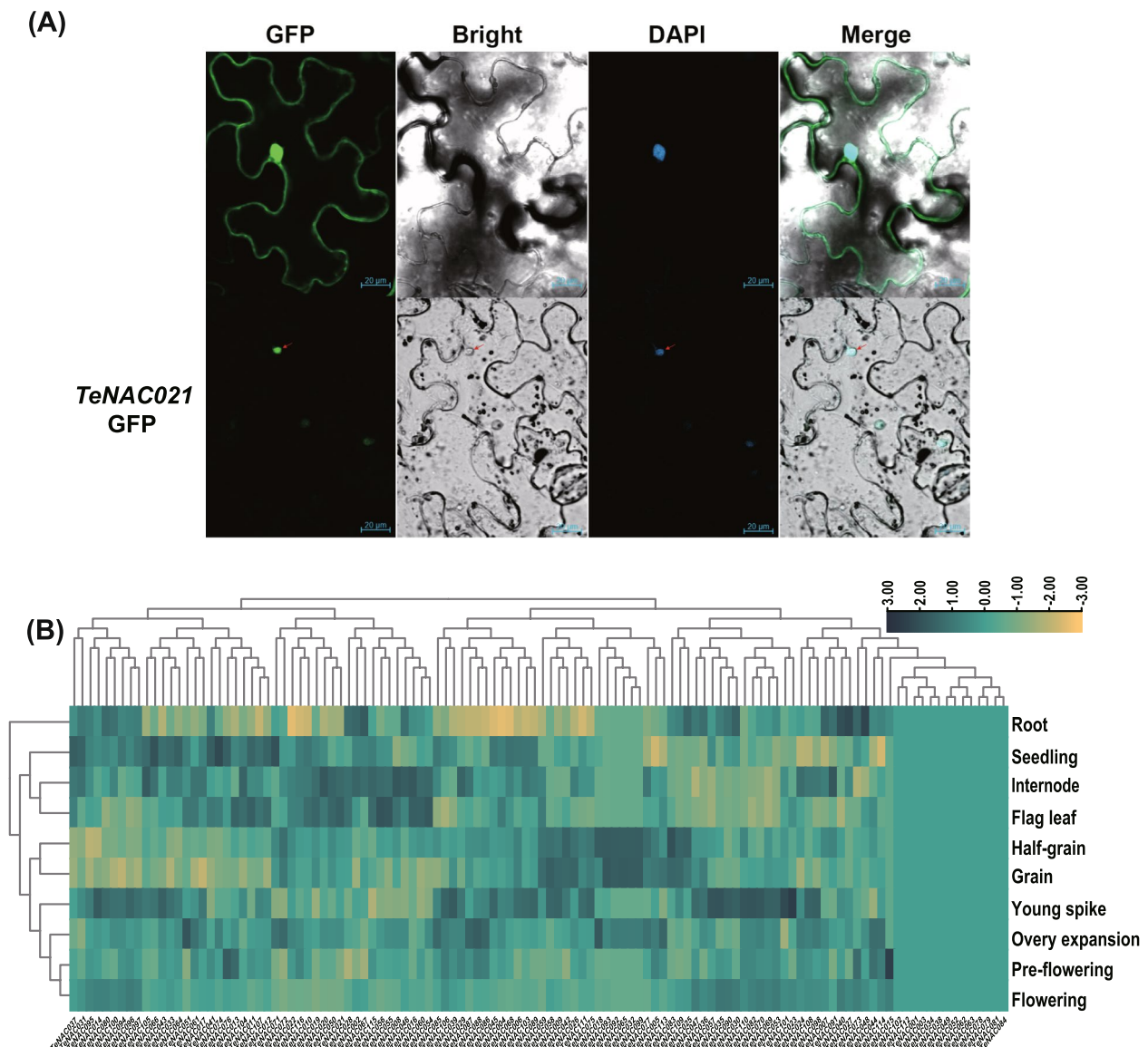


Fig. 4 The analysis of Subcellular Localization and Expression Patterns in Tissues. **A** Subcellular localization experiment, GFP represents the position of the protein under green fluorescence, Bright represents the normal light, DAPI stands for DNA stain, and Merge Indicates the result of merging GFP, Bright and DAPI **(B)** *TeNACs* in seedling, root, internode, flag leaf, young spike, pre-flowering, flowering, ovary expansion, half-grain, grain log₂ TPM in ten parts of organism and developmental period by z-score normalization

for the specific genes analyzed (Fig. 5C-J). A high degree of similarities among these eight genes, the salt-responsive gene *TaNAC29* (*TraesCS2A02G102000*) and the ABA signaling pathway gene *TaNAC48* (*TraesCS1B02G274300*) in wheat, indicating similar functions in *Th. elongatum* (Supplementary Table 8) [33, 34].

Discussion

As plant-specific transcription factors, NAC proteins play crucial roles in regulating plant growth, development, and abiotic stress responses. Currently, genome-wide identification of NAC transcription factors has been completed

in multiple species including *A. thaliana*, *O. sativa*, and *T. aestivum*; nevertheless, the NAC gene family in *Th. elongatum* has not yet been characterized [35, 36]. In this study, 116 *TeNACs*, each containing a conserved NAM domain (PF02365), were identified through comprehensive bioinformatics analysis in *Th. elongatum*. Conserved motif examination demonstrated that the seven characteristic motifs in *TeNACs* were predominantly clustered at the N-terminus following a specific arrangement (motifs 3, 4, 1, 5, 6, 2, and 7), while showing limited distribution at the C-terminus; this pattern aligns with the established NAC family features of highly conserved N-terminal domains

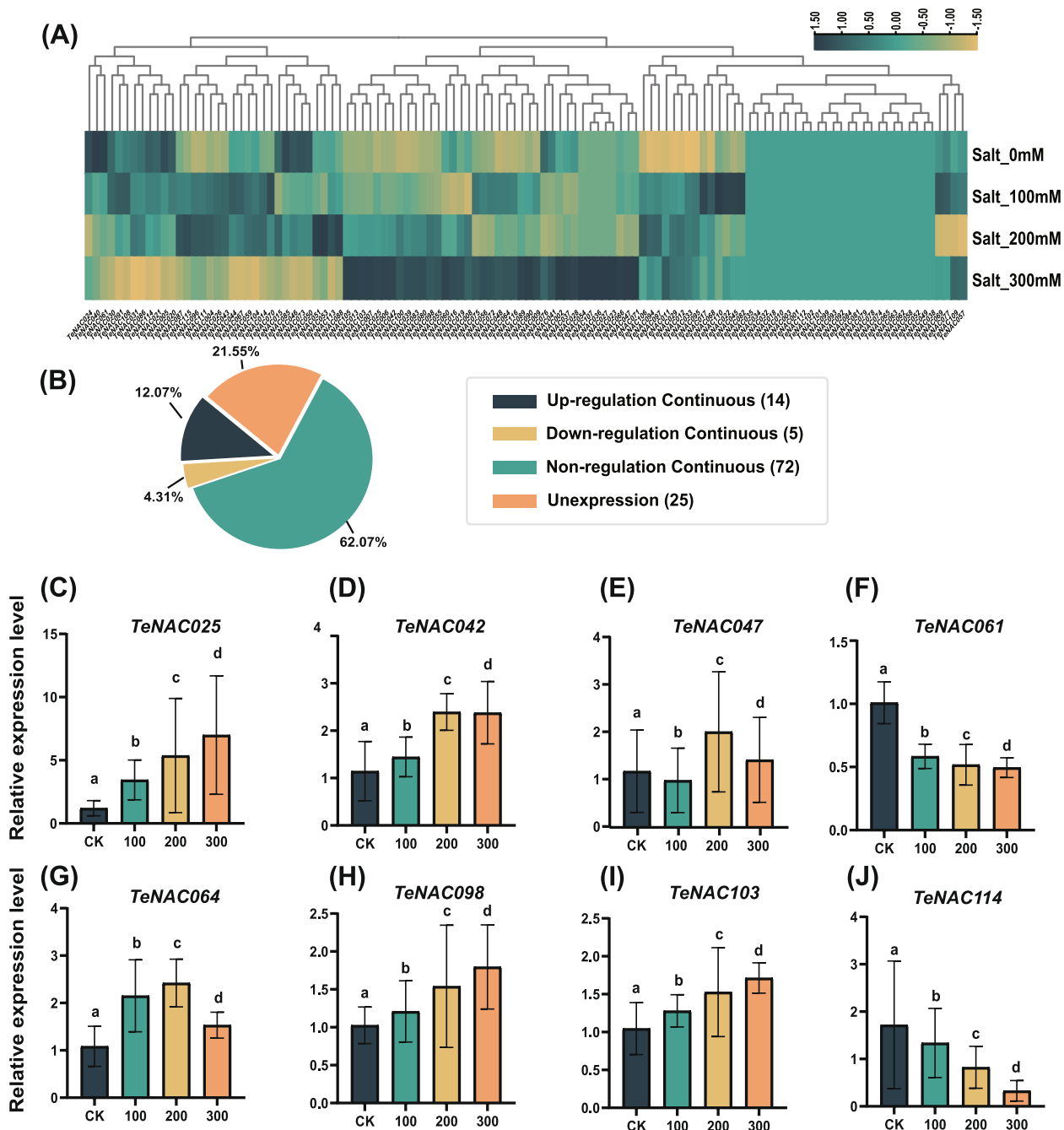


Fig. 5 Expression Analysis and RT-qPCR of *TeNACs* under Salt Stress. **A** The log₂ TPM of *TeNACs* in 0–300 mM four salt concentrations by z-score normalization. **B** Expression characteristics of *TeNACs* in four salt concentration gradients from 0 to 300 mM NaCl. **C–J** The RT-qPCR verification of 8 *TeNACs* in different salt concentrations (CK stands for 0 mM NaCl and 100–300 stands for 100 mM, 200 mM, and 300 mM NaCl respectively)

and variable C-terminal regions [37]. Furthermore, motifs 3, 4, 1, 2, and 7 were found to correspond precisely to NAC subdomains A–E, confirming the conserved domain architecture characteristic of NAC transcription factors [38]. In addition, gene structure analysis revealed that the number of exons in *TeNACs* ranged from 2 to 7, with large

differences in the number of members, indicating gene structure changes with the environment during plant growth and development [39].

Collinearity analysis identified 70, 65, and 66 orthologous gene pairs between *TeNACs* and wheat (*T. aestivum*) subgenomes A, B, and D, respectively, demonstrating high

evolutionary conservation between *TeNACs* and the wheat genome. Intraspecific collinearity analysis indicated that gene duplication events significantly contributed to *TeNAC* family expansion. Chromosomal distribution analysis revealed multiple tandemly duplicated gene pairs among *TeNAC* members, highlighting the crucial role of tandem duplications in *TeNACs* family evolution and diversification. In this study, the *TeNACs* and *Arabidopsis* NAC gene families were phylogenetically classified into 14 clusters based on conserved NAC sequences, and collinearity analysis revealed the absence of syntenic relationships between 11 *AtNACs* and *Th. elongatum* genomic fragments, suggesting evolutionary loss of two clusters. The *TeNAC* members in the same cluster shared similar gene structures and conserved motifs, among which two clusters, ANAC001 and OsNAC8, were absent in *Th. elongatum*. Protein interaction network prediction analysis based on *T. aestivum* revealed that *TeNACs* have a complex interaction network. Subcellular localization prediction revealed that except for *TeNAC021*, which may be localized in the chloroplasts or nucleus, 115 *TeNAC* members were localized in the nucleus. We experimentally verified *TeNAC021* and found that it is localized in the nucleus, so the combination of prediction and validation experiments can prove that *TeNACs021* mainly plays a major role in the nucleus.

Salt stress is a major limiting factor for plant growth [40], and several NAC gene families, including *MusaNAC042* in bananas (*Musa nana*), *AvNAC030* in kiwifruit (*Actinidia chinensis* Planch), and *TaNAC29* in *T. aestivum*, are well characterized for salt stress resistance [41, 42]. In total, 14 consistently upregulated and 5 consistently downregulated *TeNAC* members were identified when analyzing the expression pattern of *TeNAC* transcription factors in different salt stress environments; at the same time, 111 upstream *TeNACs* gene members harbored 477 ABRE cis-acting elements, and 75 members contained 116 MBS and salt stress-responsive cis-acting elements; this confirms the positive role of the NAC family in responding to salt stress and provides a reference for determining the function of NAC transcription factors and the mechanism underlying salt tolerance [43, 44]. In addition, several genes with significantly different expression genes were identified under varying salt stress conditions. Furthermore, these genes show a certain degree of orthologs with the wheat genes *TaNAC29* and *TaNAC48* [33, 34]. Combined with the abovementioned results, we hypothesized that NAC transcription factors are responsive to salt stress in *Th. elongatum*. The molecular implications of salt-responsive *TeNACs* have been expanded to address conserved regulatory mechanisms, including ROS detoxification cascades (e.g., peroxidase activation), ion transporter modulation (SOS1/NHX1 coordination), and ABA-mediated stress signaling cross-talk. Testable

hypotheses regarding cytoskeletal reorganization and cell wall remodeling under osmotic stress are proposed, with suggested validation pathways such as heterologous expression assays in *Arabidopsis* mutants or CRISPR-Cas9-mediated knockouts [45]. Expression pattern analysis of *TeNAC* members across various tissues revealed distinct expression profiles for each member in different tissue types. Sixty-nine *TeNAC* members showed detectable expression in ten examined tissues of *Th. elongatum*—including seedling, root, internode, flag leaf, young spike, pre-flowering spike, flowering stage, ovary expansion phase, half-grain, and grain—demonstrating that NAC transcription factors actively participate in plant growth and developmental processes [46]. In this study, three genes, namely, *TeNAC073*, *TeNAC044*, and *TeNAC048*, were significantly expressed under both salt stress conditions and during plant growth and development, suggesting the functional diversity of NAC transcription factors [47].

Conclusions

In this study, we employed comprehensive bioinformatics approaches to systematically investigate and predict various characteristics of the *TeNACs* family, including physicochemical properties, gene structure, conserved motifs, evolutionary relationships, collinearity patterns, protein–protein interaction networks, and expression profiles. Our analysis revealed that *TeNAC* proteins display diverse physicochemical features, contain the five characteristic NAC subdomains (A–E), and cluster into 12 distinct subfamilies that show strong collinearity with wheat NAC genes. Notably, *TeNACs* demonstrate both significant up-regulation and down-regulation under salt stress and exhibit widespread expression across different *Th. elongatum* tissues. These findings establish a solid foundation for further exploration of the biological functions and molecular mechanisms of the *TeNAC* gene family.

Supplementary Information

The online version contains supplementary material available at <https://doi.org/10.1186/s12870-025-06696-3>.

Supplementary Material 1: Supplementary Table 1. Primers used in RT-qPCR experiments. Supplementary Table 2. The protein sequences of *TeNACs*. Supplementary Table 3. The physicochemical properties of *TeNACs*. Supplementary Table 4. The protein-protein interactions of *TeNACs*. Supplementary Table 5. The log₂ TPM of *TeNACs* expression in different tissues. Supplementary Table 6. The log₂ TPM of *TeNACs* expression under salt stress. Supplementary Table 7. The p-values of differentially expressed *TeNACs* under salt stress conditions. Supplementary Table 8. The blast output of *TeNACs* in combination with *TaNAC29* and *TaNAC48*.

Supplementary Material 2: Supplementary Fig. 1. The 10 conserved motifs sequence of *TeNACs*.

Supplementary Material 3: Supplementary Fig. 2. The collinearity of 11 ANACs between *Th. elongatum* and *A. thaliana*.

Acknowledgements

We thank China Perennial Wheat Wild Relatives Germplasm Field Repository for providing the *Th. elongatum* germplasm resources.

Authors' contributions

L.H and S.L.S designed the research and experiment; J.L.S, X.C.C, J.Q.Z, F.S.M, and J.G.L performed the experiment and analyzed the data; S.H.Z provided materials; J.L.S and X.C.C prepared the original draft; S.L.S, P.Z, C.A.W and L.H revised the manuscript. All authors contributed to the article and approved the submitted version.

Funding

This work was supported by the Key R&D Program of Shandong Province, China (2023LZGC022).

Data availability

The transcriptome data used in this study have been uploaded to NCBI under BioProjectID PRJNA540081 (<https://www.ncbi.nlm.nih.gov/sra/PRJNA540081>).

Declarations

Ethics approval and consent to participate

Not applicable.

Consent for publication

Not applicable.

Competing interests

The authors declare no competing interests.

Author details

¹National Key Laboratory of Wheat Improvement, College of Agronomy, Shandong Agricultural University, Tai'an, Shandong 271018, China. ²National Key Laboratory of Wheat Improvement, Shandong Engineering Research Center of Plant-Microbial Restoration for Saline-Alkali Land, College of Life Sciences, Shandong Agricultural University, Tai'an 271018, China. ³National Key Facility of Crop Gene Resources and Breeding, Institute of Crop Sciences, Chinese Academy of Agricultural Sciences, Beijing 100081, China. ⁴Tai'an Academy of Agricultural Sciences, Tai'an, Shandong 271000, China.

Received: 13 February 2025 Accepted: 8 May 2025

Published online: 15 May 2025

References

1. Souer E, van Houwelingen A, Kloos D, Mol J, Koes R. The no apical meristem gene of *Petunia* is required for pattern formation in embryos and flowers and is expressed at meristem and primordia boundaries. *Cell*. 1996;85(2):159–70.
2. Aida M, Ishida T, Fukaki H, Fujisawa H, Tasaka M. Genes involved in organ separation in *Arabidopsis*: an analysis of the cup-shaped cotyledon mutant. *Plant Cell*. 1997;9(6):841–57.
3. Ooka H, Satoh K, Doi K, Nagata T, Otomo Y, Murakami K, Matsubara K, Osato N, Kawai J, Carninci P, et al. Comprehensive analysis of NAC family genes in *Oryza sativa* and *Arabidopsis thaliana*. *DNA Res*. 2003;10(6):239–47.
4. Zhu T, Nevo E, Sun D, Peng J. Phylogenetic analyses unravel the evolutionary history of NAC proteins in plants. *Evolution*. 2012;66(6):1833–48.
5. Vroemen CW, Mordhorst AP, Albrecht C, Kwaaitaal MA, de Vries SC. The CUP-SHAPED COTYLEDON3 gene is required for boundary and shoot meristem formation in *Arabidopsis*. *Plant Cell*. 2003;15(7):1563–77.
6. Guo S, Dai S, Singh PK, Wang H, Wang Y, Tan J, Wee W, Ito T. A Membrane-bound NAC-like transcription factor OsNLT5 represses the flowering in *Oryza sativa*. *Front Plant Sci*. 2018;9:555.
7. Liu GS, Li HL, Grierson D, Fu DQ. NAC transcription factor family regulation of fruit ripening and quality: a review. *Cells Basel*. 2022;11(3):525.
8. Christiansen MW, Gregersen PL. Members of the barley NAC transcription factor gene family show differential co-regulation with senescence-associated genes during senescence of flag leaves. *J Exp Bot*. 2014;65(14):4009–22.
9. Zhong R, Demura T, Ye ZH. SND1, a NAC domain transcription factor, is a key regulator of secondary wall synthesis in fibers of *Arabidopsis*. *Plant Cell*. 2006;18(11):3158–70.
10. He XJ, Mu RL, Cao WH, Zhang ZG, Zhang JS, Chen SY. AtNAC2, a transcription factor downstream of ethylene and auxin signaling pathways, is involved in salt stress response and lateral root development. *Plant J*. 2005;44(6):903–16.
11. Ju YL, Yue XF, Min Z, Wang XH, Fang YL, Zhang JX. VvNAC17, a novel stress-responsive grapevine (*Vitis vinifera* L.) NAC transcription factor, increases sensitivity to abscisic acid and enhances salinity, freezing, and drought tolerance in transgenic *Arabidopsis*. *Plant Physiol Biochem*. 2020;146:98–111.
12. Diao P, Chen C, Zhang Y, Meng Q, Lv W, Ma N. The role of NAC transcription factor in plant cold response. *Plant Signal Behav*. 2020;15(9):1785668.
13. Mao H, Li S, Chen B, Jian C, Mei F, Zhang Y, Li F, Chen N, Li T, Du L, et al. Variation in cis-regulation of a NAC transcription factor contributes to drought tolerance in wheat. *Mol Plant*. 2022;15(2):276–92.
14. Yuan X, Wang H, Cai J, Bi Y, Li D, Song F. Rice NAC transcription factor ONAC066 functions as a positive regulator of drought and oxidative stress response. *Bmc Plant Biol*. 2019;19(1):278.
15. Wang M, Ren LT, Wei XY, Ling YM, Gu HT, Wang SS, Ma XF, Kong GC. NAC transcription factor TwNAC01 positively regulates drought stress responses in *Arabidopsis* and triticale. *Front Plant Sci*. 2022;13:877016.
16. Yong Y, Zhang Y, Lyu Y. A Stress-Responsive NAC transcription factor from tiger lily (*LINAC2*) interacts with LIDREB1 and LIZHFD4 and enhances various abiotic stress tolerance in *Arabidopsis*. *Int J Mol Sci*. 2019;20(13):3225.
17. Xu Z, Gongbuzhaxi, Wang C, Xue F, Zhang H, Ji W. Wheat NAC transcription factor TaNAC29 is involved in response to salt stress. *Plant Physiol Biochem*. 2015;96:356–63.
18. Ren Y, Huang Z, Jiang H, Wang Z, Wu F, Xiong Y, Yao J. A heat stress responsive NAC transcription factor heterodimer plays key roles in rice grain filling. *J Exp Bot*. 2021;72(8):2947–64.
19. Zhang X, Long Y, Chen X, Zhang B, Xin Y, Li L, Cao S, Liu F, Wang Z, Huang H, et al. A NAC transcription factor OsNAC3 positively regulates ABA response and salt tolerance in rice. *Bmc Plant Biol*. 2021;21(1):546.
20. Li M, Chen R, Jiang Q, Sun X, Zhang H, Hu Z. GmNAC06, a NAC domain transcription factor enhances salt stress tolerance in soybean. *Plant Mol Biol*. 2021;105(3):333–45.
21. Baker L, Grewal S, Yang CY, Hubbart-Edwards S, Scholefield D, Ashling S, Burridge AJ, Przewieslik-Allen AM, Wilkinson PA, King IP, et al. Exploiting the genome of *Thinopyrum elongatum* to expand the gene pool of hexaploid wheat. *Theor Appl Genet*. 2020;133(7):2213–26.
22. Dai Y, Huang S, Sun G, Li H, Chen S, Gao Y, Chen J. Origins and chromosome differentiation of *Thinopyrum elongatum* revealed by *PepC* and *Pgk1* genes and ND-FISH. *Genome*. 2021;64(10):901–13.
23. Wilkins MR, Gasteiger E, Bairoch A, Sanchez JC, Williams KL, Appel RD, Hochstrasser DF. Protein identification and analysis tools in the ExPASy server. *Methods Mol Biol*. 1999;112:531–52.
24. Chen C, Hao C, Yi Z, Hannah RT, Margaret HF, Yehua H, Rui X. TBtools: an integrative toolkit developed for interactive analyses of big biological data. *Mol Plant*. 2020;13(8):1194–202.
25. Bailey TL, Boden M, Buske FA, Frith M, Grant CE, Clementi L, Ren J, Li WW, Noble WS. MEME SUITE: tools for motif discovery and searching. *Nucleic Acids Res*. 2009;37(Web Server issue):W202–8.
26. Szklarczyk D, Kirsch R, Koutrouli M, Nastou K, Mehryary F, Hachilif R, Gable AL, Fang T, Doncheva NT, Pyysalo S, et al. The STRING database in 2023: protein-protein association networks and functional enrichment analyses for any sequenced genome of interest. *Nucleic Acids Res*. 2023;51(D1):D638–46.
27. Katoh K, Standley DM. MAFFT multiple sequence alignment software version 7: improvements in performance and usability. *Mol Biol Evol*. 2013;30(4):772–80.
28. Minh BQ, Schmidt HA, Chernomor O, Schrempf D, Woodhams MD, von Haeseler A, Lanfear R. IQ-TREE 2: new models and efficient methods for phylogenetic inference in the genomic era. *Mol Biol Evol*. 2020;37(5):1530–4.
29. Chou KC, Shen HB. Cell-PLoc: a package of Web servers for predicting subcellular localization of proteins in various organisms. *Nat Protoc*. 2008;3(2):153–62.
30. Wingett SW, Andrews S. FastQ Screen: a tool for multi-genome mapping and quality control. *F1000Res*. 2018;7:1338.

31. Kim D, Langmead B, Salzberg SL. HISAT: a fast spliced aligner with low memory requirements. *Nat Methods*. 2015;12(4):357–60.
32. Anders S, Pyl PT, Huber W. HTSeq—a Python framework to work with high-throughput sequencing data. *Bioinformatics*. 2015;31(2):166–9.
33. Huang Q, Wang Y, Li B, Chang J, Chen M, Li K, Yang G, He G. TaNAC29, a NAC transcription factor from wheat, enhances salt and drought tolerance in transgenic *Arabidopsis*. *Bmc Plant Biol*. 2015;15:268.
34. Chen J, Gong Y, Gao Y, Zhou Y, Chen M, Xu Z, Guo C, Ma Y. TaNAC48 positively regulates drought tolerance and ABA responses in wheat (*Triticum aestivum* L.). *Crop J*. 2021;9(04):785–93.
35. Nuruzzaman M, Manimekalai R, Sharoni AM, Satoh K, Kondoh H, Ooka H, Kikuchi S. Genome-wide analysis of NAC transcription factor family in rice. *Gene*. 2010;465(1–2):30–44.
36. Ma J, Yuan M, Sun B, Zhang D, Zhang J, Li C, Shao Y, Liu W, Jiang L. Evolutionary divergence and biased expression of NAC transcription factors in hexaploid bread wheat (*Triticum aestivum* L.). *Plants (Basel)*. 2021;10(2):382.
37. Christianson JA, Dennis ES, Llewellyn DJ, Wilson IW. ATAF NAC transcription factors: regulators of plant stress signaling. *Plant Signal Behav*. 2010;5(4):428–32.
38. Ernst HA, Olsen AN, Larsen S, Lo LL. Structure of the conserved domain of ANAC, a member of the NAC family of transcription factors. *Embo Rep*. 2004;5(3):297–303.
39. Li C, Zhang J, Zhang Q, Dong A, Wu Q, Zhu X, Zhu X. Genome-wide identification and analysis of the NAC transcription factor gene family in garden asparagus (*Asparagus officinalis*). *Genes (Basel)*. 2022;13(6):976.
40. van Zelm E, Zhang Y, Testerink C. Salt tolerance mechanisms of plants. *Annu Rev Plant Biol*. 2020;71:403–33.
41. Tak H, Negi S, Ganapathi TR. Banana NAC transcription factor MusaNAC042 is positively associated with drought and salinity tolerance. *Protoplasma*. 2017;254(2):803–16.
42. Li M, Wu Z, Gu H, Cheng D, Guo X, Li L, Shi C, Xu G, Gu S, Abid M, et al. AvNAC030, a NAC domain transcription factor, enhances salt stress tolerance in kiwifruit. *Int J Mol Sci*. 2021;22(21):11897.
43. Yu Z, Duan X, Luo L, Dai S, Ding Z, Xia G. How plant hormones mediate salt stress responses. *Trends Plant Sci*. 2020;25(11):1117–30.
44. Dai JL, He YJ, Chen HH, Jiang JG. Dual roles of two malic enzymes in lipid biosynthesis and salt stress response in *Dunaliella salina*. *J Agric Food Chem*. 2023;71(45):17067–79.
45. Liang X, Li J, Yang Y, Jiang C, Guo Y. Designing salt stress-resilient crops: current progress and future challenges. *J Integr Plant Biol*. 2024;66(3):303–29.
46. Wang J, Wang H, Yang H, Hu R, Wei D, Tang Q, Wang Z. The role of NAC transcription factors in flower development in plants. *Sheng Wu Gong Cheng Xue Bao*. 2022;38(8):2687–99.
47. Olsen AN, Ernst HA, Leggio LL, Skriver K. NAC transcription factors: structurally distinct, functionally diverse. *Trends Plant Sci*. 2005;10(2):79–87.

Publisher's Note

Springer Nature remains neutral with regard to jurisdictional claims in published maps and institutional affiliations.